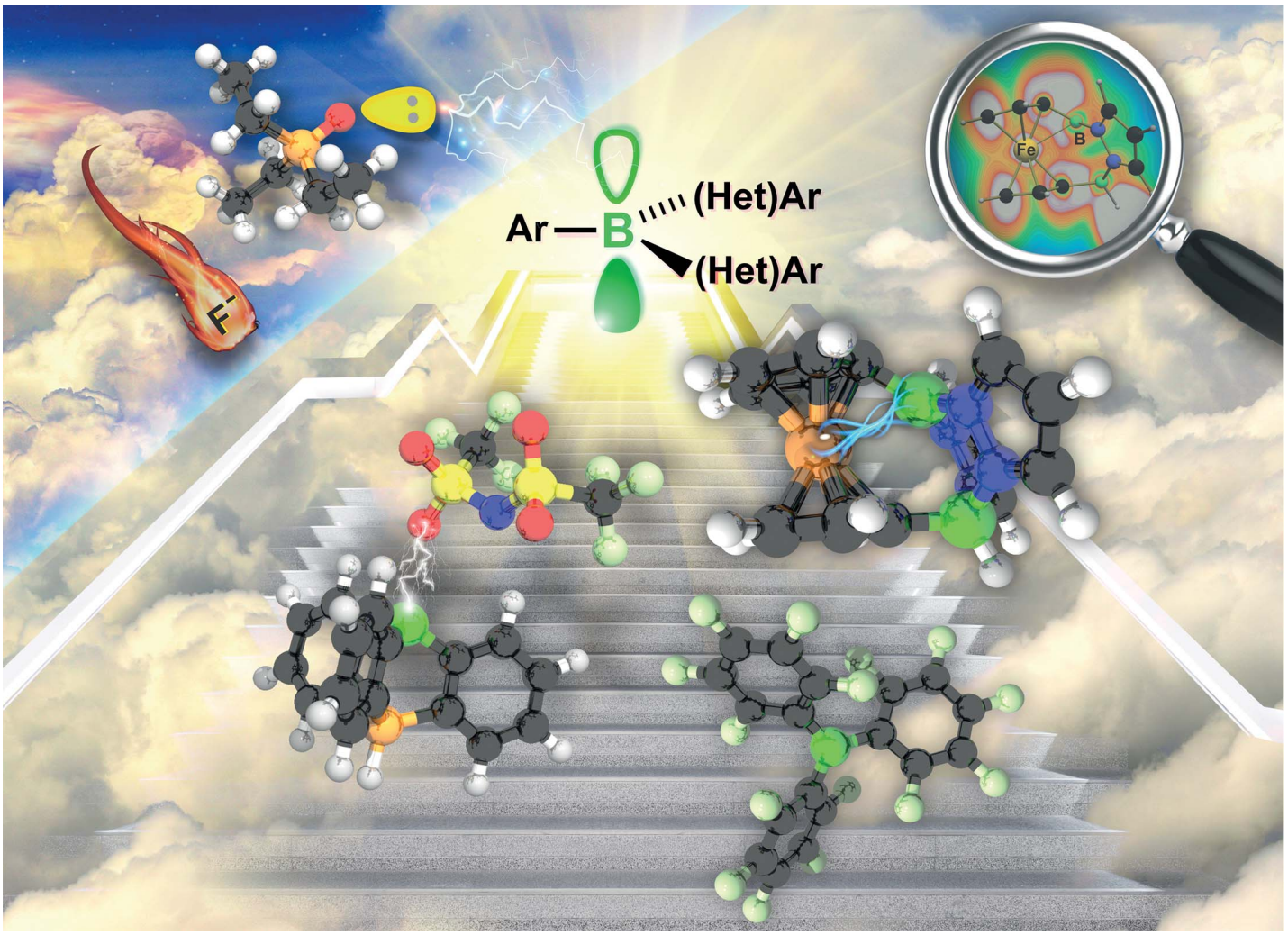

Showcasing research from Dr. Peter Hrobárik's laboratory, Faculty of Natural Sciences, Comenius University in Bratislava, Slovakia and Prof. Matthias Wagner's laboratory, Goethe University Frankfurt, Germany.

A free boratriptycene-type Lewis superacid

By exploiting the facile self-assembly of the pyrazabole scaffold, authors have devised a straightforward route to boratriptycene-type precursors that have two pyrazole bridges and one 1,1'-ferrocenylene linker between two bridgehead BH moieties. Single hydride abstraction generates ferrocene-stabilized borenium cations with an unprecedentedly large dip angle and exceptional Lewis acidity that can nevertheless be isolated in free form. Exceptional acidity of the prepared borenium salts stems from the structural strain imparted by the bridging rigid pyrazabole moieties, while weak Fe(3d)→B(2p) bonding prevents the planar borenium center from interaction with weakly-coordinated counterions.

As featured in:

See Peter Hrobárik, Matthias Wagner *et al.*, *Chem. Sci.*, 2022, **13**, 1608.

ROYAL SOCIETY OF CHEMISTRY

rsc.li/chemical-science

Registered charity number: 207890

Chemical Science

ROYAL SOCIETY OF CHEMISTRY

EDGE ARTICLE

View Article Online
View Journal | View Issue

Check for updates

Cite this: *Chem. Sci.*, 2022, **13**, 1608

All publication charges for this article have been paid for by the Royal Society of Chemistry

Received 17th November 2021
Accepted 5th December 2021

DOI: 10.1039/d1sc06404e

rsc.li/chemical-science

A free boratriptycene-type Lewis superacid†

Marcel Henkelmann,[a] Andreas Omlor,[b] Michael Bolte,[a] Volker Schünemann,[b] Hans-Wolfram Lerner,[a] Jozef Noga,[c] Peter Hrobárik *[c] and Matthias Wagner *[a]

Bicyclic pyrazabole-bridged ferrocenes with BH groups at their bridgehead positions were prepared from $[Li(thf)]_2[1,1'\text{-fc}(BH_3)_2]$ and pyrazole or 3,5-dimethylpyrazole in the presence of Me_3SiCl (**1** or **1Me**, respectively; 1,1′-fc = 1,1′-ferrocenylene); Me_3SiH and H_2 are released as byproducts. Treatment of **1** or **1Me** with 1 eq. of the hydride scavenger $[Ph_3C][B(C_6F_5)_4]$ afforded the borenium salts $[\mathbf{2}][B(C_6F_5)_4]$ (72%) and $[\mathbf{2Me}][B(C_6F_5)_4]$ (77%). According to X-ray crystallography, $[\mathbf{2Me}]^+$ contains one trigonal-planar borenium cation, the cyclopentadienyl (Cp) rings of the 1,1′-fc fragment remain parallel to each other, but the Cp–B bond vector is bent out of the Cp plane by an unprecedentedly large dip angle α^* of 40.6°. The Fe···B(sp^2) distance is very short (2.365(4) Å) and the ^{11}B NMR signal of the cationic B(sp^2) center is remarkably upfield shifted (23.4 ppm), suggesting a direct Fe(3d) → B(2p) donor–acceptor interaction. Although this interpretation is confirmed by quantum-chemical calculations, the coupling between the associated orbitals corresponds to an energy of only 12 kJ mol^{-1}. Accordingly, both the experimental (*e.g.*, Gutmann–Beckett acceptor number AN = 111) and theoretical assessment (*e.g.*, Et_3PO and F^--ion affinities) of the Lewis acidity proves that $[\mathbf{2}]^+$ is among the strongest boron-based Lewis acids available to date.

Introduction

The rise to prominence of boron-based Lewis acids began when their application potential as activators for metal-catalyzed homogeneous olefin polymerization was recognized.[1] The advent of the 'Frustrated Lewis Pairs' led to a further surge of interest, which has remained at a high level ever since.[1,2] Among all the remarkable developments in the field, we focus here particularly on Lewis acidic organoboranes ('Lewis superacids').[3]

One way to increase the affinity of a triorganylborane (BR_3) for even weak Lewis bases is to introduce electronegative halogen substituents at the periphery.[4] Classic examples include the compounds $B(C_6F_5)_3$ of Massey and Park[5] or $B(C_6Cl_5)_3$ of Ashley and O'Hare.[6] As an alternative, mesomerically electron-withdrawing substituents have also been employed.[7] The affinity of a boron center (in particular) for anionic ligands can also be increased by the Coulomb attraction of an adjacent positively charged group.[8] Gabbaï *et al.* took advantage of this effect when they used the phosphonium borane ($[\mathbf{A}]^+$; Fig. 1) to bind F^- ions in water despite their high hydration enthalpy.[9,10] Our group combined a high fluorine load with the positive charge of a phosphonium center to create a Lewis acid $[\mathbf{B}]^+$, stronger than $B(C_6F_5)_3$ and suitable as a catalyst for Diels–Alder

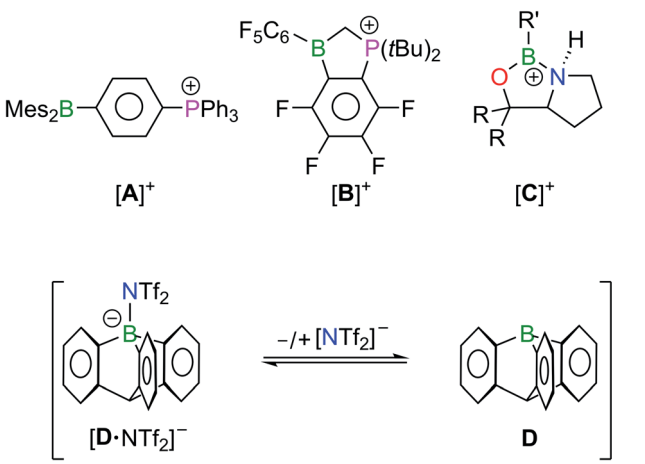

Fig. 1 Organoboranes of particularly high Lewis acidity due to introduced positive charges and fluorine substituents ($[\mathbf{A}]^+$, $[\mathbf{B}]^+$, $[\mathbf{C}]^+$) or structurally enforced pyramidalization (**D**). Mes = 2,4,6-$Me_3C_6H_2$, Tf = O_2SCF_3.

[a]*Institute of Inorganic Chemistry, Goethe University Frankfurt, Max-von-Laue-Straße 7, 60438 Frankfurt am Main, Germany. E-mail: matthias.wagner@chemie.uni-frankfurt.de*

[b]*Physics Department, University Kaiserslautern, Erwin-Schrödinger-Straße 56, 67663 Kaiserslautern, Germany*

[c]*Department of Inorganic Chemistry, Faculty of Natural Sciences, Comenius University, Ilkovicova 6, 84215 Bratislava, Slovakia. E-mail: peter.hrobarik@uniba.sk*

† Electronic supplementary information (ESI) available: Experimental, computational, and crystallographic data. CCDC 2120063–2120067. For ESI and crystallographic data in CIF or other electronic format see DOI: 10.1039/d1sc06404e

Open Access Article. Published on 07 diciembre 2021. Downloaded on 21/04/2026 15:29:20.
This article is licensed under a Creative Commons Attribution-NonCommercial 3.0 Unported Licence.

© 2022 The Author(s). Published by the Royal Society of Chemistry

Open Access Article. Published on 07 diciembre 2021. Downloaded on 21/04/2026 15:29:20.
This article is licensed under a Creative Commons Attribution-NonCommercial 3.0 Unported Licence.

reactions.[11] By shifting the positive charge even closer to the boron center, Corey *et al.* obtained chiral oxazaborolidinium cations $[C]^+$ that serve as broadly applicable catalysts in (enantioselective) [4 + 2]- and [3 + 2]-cycloaddition reactions.[12] Most trivalent compounds BR_3 with an empty boron 2p orbital adopt trigonal planar configurations. Only after coordination of a Lewis basic donor (Do) is the BC_3 moiety pyramidalized to allow for a (distorted) tetrahedral geometry of the $BR_3{\cdot}Do$ adduct. However, when a rigid organic framework is designed to impose a structural constraint on the B atom that forces the BC_3 core out of planarity, the free Lewis acid becomes destabilized but also better preorganized for ligand coordination. As a consequence, the organoborane becomes a better electron-pair acceptor.[3a–c,13] Mikhailov realized such a structural motif by the synthesis of 1-boraadamantane,[14,15] while Berionni *et al.* released a non-planar 9-boratriptycene (**D**) by *in situ* protonolysis of corresponding borate-complexes $[R_4P][t\text{Bu}C_6H_4\text{–}\mathbf{D}]$ with $HNTf_2$ in CH_2Cl_2 ($Tf = O_2SCF_3$).[16] In the resulting mixture, **D** is in an association–dissociation equilibrium with the weakly coordinating $[NTf_2]^-$ ion and was isolated in the form of its trapping products with various N-, P-, or O-centered Lewis bases.[17] Structural data from X-ray crystallography are not available for either free 1-boraadamantane or **D**. Gas-phase electron diffraction on 3-methyl-1-boraadamantane at 100 °C revealed that the B atom in the equilibrium structure has a (slightly) pyramidal configuration with $\sum$(C–B–C) = 349.4(4)° and av. d(B–C) = 1.556(5) Å.[18] The experimentally determined structural parameters were confirmed by quantum-chemical calculations, which further indicate significant hyperconjugation between the vacant boron 2p orbital and its adjacent C–C σ bonds (average stabilization energy: 64.4 kJ mol^{-1}; electron occupancy q(B(2p)): 0.17 e^-).[18,19] Compared to 1-boraadamantane, the computed molecular structure of **D** shows a more pyramidalized BC_3 core ($\sum$(C–B–C) = 339.3°) while q(B(2p)) is lower (0.08 e^-).[16]

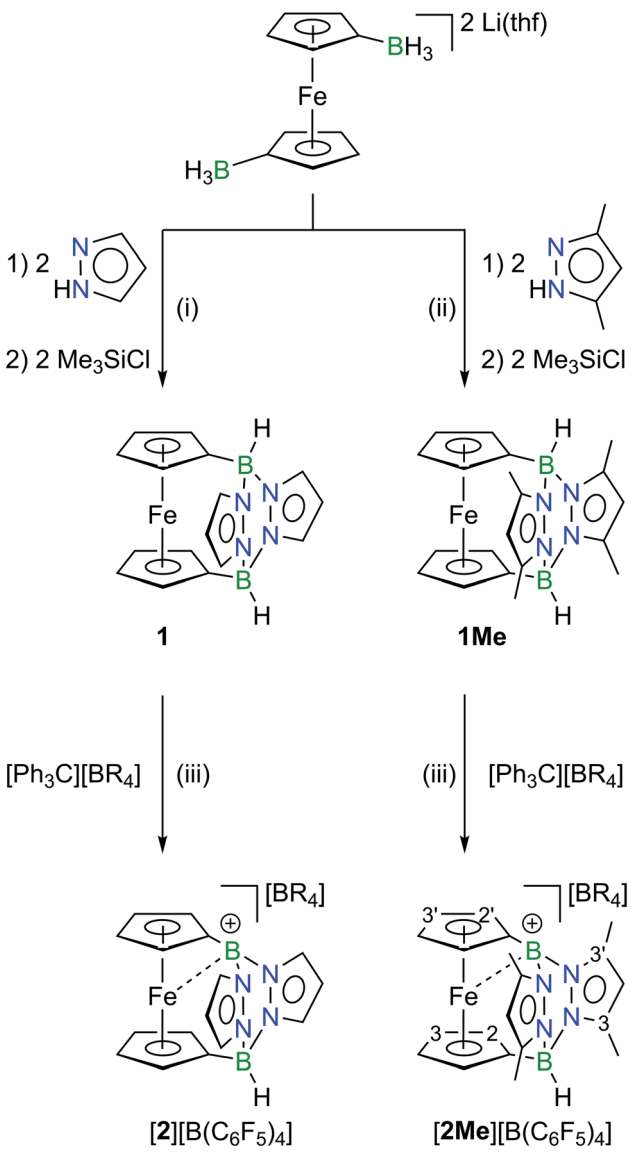

Scheme 1 Synthesis of pyrazabole-bridged *ansa*-ferrocenes **1** and **1Me**; hydride abstraction to afford the borenium-ion salts $[\mathbf{2}][B(C_6F_5)_4]$ and $[\mathbf{2Me}][B(C_6F_5)_4]$. Reagents and conditions: (i) THF, −78 °C (30 min) to 70 °C (6 h). (ii) THF, room temperature (overnight) to 70 °C (3 h). (iii) CH_2Cl_2, room temperature, 1 min. $R = C_6F_5$.

Taking into account the above developments over the last two decades, we have now designed a novel ferrocenylborane-based[10h,20,21] Lewis superacid $[\mathbf{2}]^+$ guided by the following criteria (Scheme 1): (i) facile synthesis inspired by the self-assembly of pyrazaboles or scorpionate ligands;[22] (ii) a positively charged B center with electronegative N(sp^2) atoms in its first coordination sphere, which cannot donate π-electron density to the vacant p orbital on the B atom due to the orthogonal positions of the filled p orbitals on the N atoms;[23–25] (iii) a strained scaffold analogous to boratriptycene. The 1,1′-ferrocenylene bridge in $[\mathbf{2}]^+$ has two functions to prevent the molecule from exceeding its stability limits: (i) a weak and easily displaced Fe → B^+ through-space interaction should help to buffer the electron deficiency of the free borenium cation in its resting state.[10h,20] (ii) Because of the facile distortion of the normally parallel cyclopentadienyl rings toward a tilted orientation, the 1,1′-ferrocenylene unit can act as a hinge that mitigates an overly strained pyramidal configuration of the B atom. The synthesis and key properties of $[\mathbf{2}]^+$-type compounds will be described herein.

Results and discussion

Synthesis of $[\mathbf{2}][B(C_6F_5)_4]$ and $[\mathbf{2Me}][B(C_6F_5)_4]$

Treatment of the readily available hydridoborate salt $[Li(thf)]_2[1,1'\text{-fc}(BH_3)_2]$[26] with pyrazole or 3,5-dimethylpyrazole and Me_3SiCl afforded the pyrazabole-bridged *ansa*-ferrocenes **1** and **1Me** in yields of 39% and 55%, respectively (Scheme 1; 1,1′-fc = 1,1′-ferrocenylene); Me_3SiH and H_2 are formed as the byproducts. Clean and quantitative hydride abstraction was achieved through the reaction of **1** or **1Me** with the hydride scavenger $[Ph_3C][B(C_6F_5)_4]$ in CH_2Cl_2. After precipitation with *n*-pentane, $[\mathbf{2}][B(C_6F_5)_4]$ (72%) and $[\mathbf{2Me}][B(C_6F_5)_4]$ (77%) were isolated in good yields. Crystals of the borenium salts suitable for X-ray analysis were grown by layering their concentrated solutions in CH_2Cl_2 with *n*-hexane.[27]

© 2022 The Author(s). Published by the Royal Society of Chemistry

Open Access Article. Published on 07 diciembre 2021. Downloaded on 21/04/2026 15:29:20.
This article is licensed under a Creative Commons Attribution-NonCommercial 3.0 Unported Licence.

X-ray crystallography

Both precursor/borenium-ion pairs, **1**/[**2**][$B(C_6F_5)_4$] and **1Me**/[**2Me**][$B(C_6F_5)_4$], were studied by X-ray diffraction. Since the crystal lattice of [**2**][$B(C_6F_5)_4$] contains three crystallographically independent entities in the asymmetric unit, only the molecular structures of **1Me**/[**2Me**][$B(C_6F_5)_4$] are compared here (Fig. 2). We verified that all the conclusions drawn are also valid for the pair **1**/[**2**][$B(C_6F_5)_4$] (see the ESI†).

The 1,1′-ferrocenylene moieties in **1Me**/[**2Me**]$^+$ adopt almost perfectly staggered conformations with torsion angles $C_i - COG - COG' - C_i'$ close to zero (C_i = B-bonded C atom; COG = cyclopentadienyl-ring centroid). No significant differences are also observed between the B–C (av. 1.596 Å) or B–N (av. 1.567 Å) bond lengths in **1Me** and the B(2)–C (1.613(6) Å) or B(2)–N (av. 1.568 Å) bond lengths in [**2Me**]$^+$. The configuration of the second B atom, however, changes fundamentally from tetrahedral to trigonal-planar upon going from **1Me** to [**2Me**]$^+$ (sum of angles around B(1) = 359.7°). Accordingly, the B(1)–C (1.497(6) Å) and B(1)–N (av. 1.506 Å) bonds of [**2Me**]$^+$ are contracted relative to the corresponding bonds at B(2). This contraction is about twice as pronounced for B(1)–C (Δ = 0.116 Å) as for B(1)–N (Δ = 0.062 Å). The B(1)–C bond of [**2Me**]$^+$ is also considerably shorter than the exocyclic B–C bond between the orthogonally positioned planes in 9-Mes-9-borafluorene (1.562 Å), which we take as an archetypal B(sp^2)–C(sp^2) single bond.[28] The B(1)–N bonds of [**2Me**]$^+$ are still longer than the average B–N bond in propeller-shaped $B(pyrMe_2)_3$ (1.443 Å; $pyrMe_2$ = 2,5-dimethylpyrrolyl), for which B=N π bonding is negligible.[29] The most important structural features of [**2Me**]$^+$ are the pronounced dip angle α^* = 40.6° and the short Fe···B(sp^2) contact of 2.365(4) Å ($\alpha^* = 180° - \alpha$; α = COG–C_i–B(1)). Corresponding distortions have already been observed for other ferrocenylboranes, but the dip angles are much smaller even in the most extreme cases, *i.e.*, $FcBBr_2$: α^* = 18.9°,[20a] 9-Fc-9-borafluorene: α^* = 25.5°,[20d] $FcBC_4Ph_4$: α^* = 29.4° (Fc = ferrocenyl).[20f] The planarization of one bridgehead B atom does not result in a substantial tilting of the ferrocenylene unit: **1Me**/[**2Me**]$^+$ show largely coplanar cyclopentadienyl rings with Cp//Cp′ angles of 5.2(2)/5.4(2)°. The 'hinge-effect' of the 1,1′-fc bridge, which was assumed in the design of the molecular framework, obviously does not play a major role. Considerable differences are observed for the pyrazabole moieties of **1Me** *vs.* [**2Me**]$^+$: the gap between the two pyrazol-1-yl (pz) rings is significantly wider in **1Me** than in [**2Me**]$^+$ (pz//pz′ = 146.8(1)° *vs.* 118.7(2)°) and the dihedral angle between the best plane through the four N atoms and the B(2)-bonded Cp ring amounts to a value of 88.3° in **1Me**, but only to 71.6° in [**2Me**]$^+$.

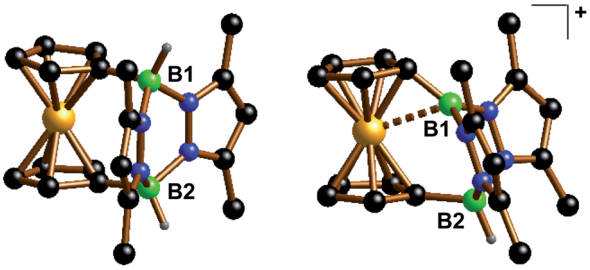

parameter	**1Me**	[**2Me**][$B(C_6F_5)_4$]
B(1)–C [Å]	1.593(3)	1.497(6)
B(2)–C [Å]	1.598(3)	1.613(6)
B(1)–N [Å]	1.565(2)	1.505(5)
	1.568(2)	1.506(5)
B(2)–N [Å]	1.562(2)	1.566(6)
	1.570(2)	1.569(6)
Fe···B(1) [Å]	3.241(2)	2.365(4)
α^* [°]	1.6	40.6

Fig. 2 Molecular structures of **1Me** (left) and [**2Me**][$B(C_6F_5)_4$] (right) in the solid state. C-bonded H atoms and the $[B(C_6F_5)_4]^-$ anion are omitted for clarity. Selected structural parameters are compiled in the table.

NMR spectroscopy

NMR spectra were recorded in $CDCl_3$ or CD_2Cl_2. The changes in the ^{1}H, ^{11}B, and ^{13}C{^{1}H} NMR spectra upon going from **1** to [**2**]$^+$ or **1Me** to [**2Me**]$^+$ are very similar and will be discussed here exemplarily for the **1Me**/[**2Me**]$^+$ pair.

The ^{11}B NMR spectrum of the precursor molecule **1Me** shows a resonance in the typical region of tetracoordinated boron nuclei (−7.6 ppm).[30] After H^- abstraction, the spectral parameters of the residual BH moiety of [**2Me**]$^+$ remain largely the same, whereas the newly generated cationic B center gives rise to a signal at 23.4 ppm. Its chemical shift is highly unusual for tricoordinated B sites, which should be much less shielded.[30] Since the formation of adduct equilibria with the weakly coordinating solvent molecules CD_2Cl_2 is unlikely (as also supported by our DFT simulations), we attribute the peculiar NMR feature either to a true Fe···B bonding interaction or to a magnetic anisotropy effect of the Fe d-electrons in close proximity to the B cation. We note in this context that upfield shifts of the ^{11}B resonances have also been observed for $FcBBr_2$ *vs.* $PhBBr_2$ (46.7 *vs.* 56.6 ppm),[31] 9-Fc-9-borafluorene *vs.* 9-Ph-9-borafluorene (53.0 *vs.* 64.5 ppm),[20d] and $FcBC_4Ph_4$ *vs.* $PhBC_4Ph_4$ (47.4 *vs.* 65.4 ppm);[20f] along this series, the shift difference increases as the dip angle α^* increases.

H^--ion abstraction leads to a symmetry breaking that renders the two Cp rings of [**2Me**]$^+$ chemically inequivalent. The assignment of resonances to Cp′–B^+ or Cp–B(H) was achieved by means of a NOESY spectrum (*cf.* Scheme 1 for the atom labeling): an intense cross peak was observed between a pzCH_3 signal at $\delta(^1H)$ = 2.56 and a Cp*H* resonance at $\delta(^1H)$ = 4.11 ppm; a second, significantly weaker, cross peak was detected between the second pzCH_3 signal (2.48 ppm) and a Cp*H* resonance at 3.31 ppm (pz = pyrazol-1-yl). Through-space interactions of two nuclear spins that are in closer proximity to each other tend to result in a more pronounced NOE. Since we know from the solid-state structure of [**2Me**][$B(C_6F_5)_4$] that the average distance between Cp*H*-2′ and pz*C*H_3-3′ is 2.94 Å and thus approximately 30% shorter than the distance between Cp*H*-2 and pz*C*H_3-3 (4.19 Å), we assign the proton signals at 4.11/3.31 ppm to

© 2022 The Author(s). Published by the Royal Society of Chemistry

Open Access Article. Published on 07 diciembre 2021. Downloaded on 21/04/2026 15:29:20.
This article is licensed under a Creative Commons Attribution-NonCommercial 3.0 Unported Licence.

Cp*H*-2′/Cp*H*-2 and those at 2.56/2.48 to pzCH_3-3′/pzCH_3-3. The proton and carbon nuclei in the Cp′ ring of [**2Me**]$^+$ are considerably deshielded relative to those of **1Me** due to the electron-withdrawing effect of the attached borenium cation ($\Delta\delta$: CpH-3′ = 1.40, CpH-2′ = 0.78 ppm; CpC-3′ = 15.5, CpC-2′ = 9.3 ppm). A qualitatively similar, albeit less marked, effect is also visible for the Cp ring of [**2Me**]$^+$ *vs.* **1Me**. Also all ^{1}H and ^{13}C NMR resonances of the pyrazolyl rings of [**2Me**]$^+$ experience downfield shifts compared to the corresponding signals of **1Me**.

Dynamic hydride-exchange equilibrium between 1 and [2]$^+$

On one occasion, in the attempt to synthesize the borenium-cation salt [**2**][B(C_6F_5)$_4$], we inadvertently added only about 0.8 eq. of [Ph_3C][B(C_6F_5)$_4$] to **1** (NMR-scale experiment; CD_2Cl_2). A subsequent ^{1}H NMR spectroscopic investigation of the sample revealed well-resolved resonances of the byproduct Ph_3CH, but extremely broad signals of the ferrocene-containing species. We attributed this effect to a dynamic exchange equilibrium of hydride ions between tetracoordinated BH and tricoordinated B$^+$ sites. To test this assumption, we intentionally prepared a mixture of **1** (1.0 eq.) and [Ph_3C][B(C_6F_5)$_4$] (0.9 eq.) in CD_2Cl_2 and were able to reproduce the previous observation. After addition of [nBu$_4$N][BH_4] (1.0 eq. of the [BH_4]$^-$ ion) to the sample, sharp proton resonances of **1** reappeared. The hydride abstraction/addition sequence was accompanied by only little decomposition (mainly producing ferrocene), and the proton-integral ratios of the re-generated **1** and Ph_3CH conformed to an almost equimolar distribution (see the ESI† for plots of the spectra). In a second experiment, we prepared a 1 : 1 mixture of **1** and [**2**][B(C_6F_5)$_4$] (CD_2Cl_2); the observed ^{1}H and ^{11}B NMR resonances were broadened almost beyond detection (except for the [B(C_6F_5)$_4$]$^-$-anion signal). Upon cooling from room temperature to 243 K, the resonances became slightly sharper and the number of distinguishable signals increased as the exchange equilibrium was slowed down. We finally repeated the latter experiment with the 3,5-dimethylpyrazolyl derivatives **1Me** and [**2Me**][B(C_6F_5)$_4$]. Here, the line-broadening was much less pronounced and we were still able to identify all proton resonances of the two species in the NMR spectrum of the mixture. This result clearly shows that the introduced methyl groups provide considerable steric shielding of the boron centers, further confirming our hypothesis of a 'hydride jump' as the origin of the line-broadening effect.

Electronic structures of [2]$^+$/[2Me]$^+$ and quantum-chemical calculations

Our experimental results consistently point toward the existence of a donor–acceptor Fe(3d) → B(2p) interaction in the borenium ions [**2**]$^+$/[**2Me**]$^+$, similar to the Fe → Si$^+$ interaction in ferrocene-stabilized silylium ions.[32] Comparable interactions have been also found for complexes of so-called Z-type ligands, in which Lewis-basic metal atoms donate charge density to Lewis-acidic boron sites located in the ligand backbones.[33] Closely related examples to our system are certain metallaboratranes, *i.e.*, complexes containing κ^4-tris(2-mercaptoimidazolyl)borane ligands that interact with the coordinated metal atom *via* three dative S → M σ bonds and one retrodative M → B σ bond.[34]

The experimentally determined very short Fe⋯B$^+$ contacts in [**2**]$^+$ and [**2Me**]$^+$ (Fig. 2) are well reproduced at the DFT level (PBE-D3(BJ)/def2-TZVPP), which provides optimized Fe⋯B$^+$ distances of 2.34 Å and 2.38 Å for [**2**]$^+$ and [**2Me**]$^+$, respectively; these values are practically unaffected by considering/neglecting corrections for dispersion forces. It was also theoretically confirmed that the dip angles α* are the largest among all ferrocene-stabilized boranes or borenium ions and that they are comparable to the corresponding dip angles in [Fc–SiR_2]$^+$ cations[32] (α* = 41.9° for [**2**]$^+$ and 40.0° for [**2Me**]$^+$; Table S4†). Moreover, we found an excellent agreement between the computed and experimental ^{11}B NMR chemical shift values (Table S5 and Fig. S66†), demonstrating that the optimized/solid-state structures prevail in solution (elongated Fe⋯B$^+$ distances would result in downfield-shifted ^{11}B(sp^2) resonances).

The question now arises, to what extent the short Fe⋯B$^+$ contacts in [**2**]$^+$ and [**2Me**]$^+$ can be attributed to a 'through-space' Fe(3d) → B(2p) donor–acceptor interaction. Structural strain imparted by the bridging rigid pyrazabole moieties and the avoidance of a pyramidalized tricoordinated B(sp^2) center probably also play a role. According to an NBO second-order perturbation energy analysis, the stabilization energy $E^{(2)}$ for the coupling between the occupied 'lone-pair' orbital on Fe and the vacant B(2p) orbital corresponds to only 12 kJ mol^{-1}, which is about eight times less than the stabilization energy found for the Fe → Si$^+$ interaction in [Fc–SiR_2]$^+$ ions.[32] The relative weakness of the Fe(3d) → B(2p) interaction in [**2**]$^+$/[**2Me**]$^+$ is further indicated by the following facts: (i) the B(sp^2) center is trigonal planar rather than inwardly pyramidalized. (ii) An optimization of the model system Fc–Bpz_2, formally obtained from [**2**]$^+$ by removing the B(sp^3)H tether to the second Cp ring, leads to a notably longer Fe⋯B contact of 2.70 Å, even after protonation of the pyrazole moieties or N,N′-chelation of a [BH_2]$^+$ fragment to introduce the overall positive charge (Fig. S63†). The impact of structural strain on the Fe⋯B$^+$ distance is also evident from a comparison of the energies of [**2**]$^+$ in its optimized geometry and in a hypothetical geometry with outwardly pyramidalized borenium center and diminished Fe(3d) → B(2p) interaction ([**2**^{pyram}]$^+$; the structure was obtained from that of **1** by hydride abstraction while keeping the dihedral angle θ(N–B–N–C$_i$) fixed during the optimization; Fig. S64†). Relative to [**2**]$^+$, [**2**^{pyram}]$^+$ is energetically disfavored by 117 kJ mol^{-1}, which is much more than the stabilization energy of the Fe(3d) → B(2p) interaction. Mayer bond orders (MBO = 0.43 for [**2**]$^+$, 0.40 for [**2Me**]$^+$) and QTAIM delocalization indices (DI = 0.21 for [**2**]$^+$, 0.18 for [**2Me**]$^+$) suggest a small covalency for the 'through-space' Fe(3d) → B(2p) interaction in [**2**]$^+$ and [**2Me**]$^+$, where these parameters are about twice as large as those found for previously reported Fc–B analogues (Table S4†). The partial covalency of the Fe(3d) → B(2p) interaction in [**2**]$^+$ and [**2Me**]$^+$ is also seen in ELI-D and NLMO analyses (Fig. 3), both revealing a three-center two-electron (3c2e) bond between the Fe(II) center, the B(sp^2) cation, and the attached C$_i$ atom of the Cp ring. In the simplified Lewis structure notation, the 3c2e bond in [**2**]$^+$ and [**2Me**]$^+$ results from a sharing of the respective Fe–C$_i$ electron bonding pair, which has a large Fe(3d) character,

Open Access Article. Published on 07 diciembre 2021. Downloaded on 21/04/2026 15:29:20.
This article is licensed under a Creative Commons Attribution-NonCommercial 3.0 Unported Licence.

with the vacant B(2p) orbital. The 3c2e bond thus can be viewed as a donor–acceptor interaction (see Fig. 3b for the composition of corresponding NLMO orbitals). In contrast, the corresponding 3c2e bond in structurally related $[Fc–SiR_2]^+$ ions is formed with the C_i atom of the other Cp ring. This difference might be attributed to the larger covalent/ionic radii of tricoordinated Si^+ compared to tricoordinated B^+ ions.

The metal → B interaction found for $[\mathbf{2}]^+$ is computed to become significantly stronger when the Fe(II) center in the metallocene scaffold is replaced by heavier Ru(II) or Os(II) ions with more diffuse 4d or 5d valence orbitals, respectively. This is concluded mainly from the shorter $M\cdots B^+$ contacts (M = Ru, Os) despite the larger ionic radii of these M(II) centers, and also from the larger $M\cdots B^+$ covalency revealed by the larger QTAIM delocalization indices and Mayer bond orders (Table S4†).

Despite the existing Fe(3d) → B(2p) interaction and a hence conceivable charge transfer leading to the generation of Fe(III)/B$^\bullet$ radical pairs, the electronic ground states of $[\mathbf{2}]^+$ and $[\mathbf{2Me}]^+$ remain diamagnetic with Fe(II) and B^+ centers, which is confirmed by computed and experimental NMR shifts as well as ^{57}Fe Mössbauer spectral parameters (Fig. S51, S52 and Tables S1, S6†). The electron-spin density in the lowest-lying triplet state of $[\mathbf{2}]^+$ (147 kJ mol^{-1} above the singlet ground state) resides almost exclusively on the Fe(II) center, with just small positive/negative fractions at the C atoms of both Cp rings (Fig. S65†). The same holds for higher-lying triplet excited states and thus, even upon singlet-triplet excitation, the Fe(3d) → B(2p) interaction would not be expected to promote the formation of an Fe(III)/B$^\bullet$ radical pair. A qualitatively similar picture, but with notably larger energy gap between singlet and triplet states, is obtained for the ruthenocene analogue of $[\mathbf{2}]^+$ (ΔE = 280 kJ mol^{-1}). In striking contrast, the osmocene congener (which is also predicted to feature a singlet ground state with Os(II) and B^+ centers) is computed to display a distinct Os(III)/B$^\bullet$ character in its relaxed triplet excited state (ΔE = 238 kJ mol^{-1}).

Finally, we propose that the Fe(3d) → B(2p) interaction in $[\mathbf{2}]^+/[\mathbf{2Me}]^+$, while not significantly reducing the Lewis acidity of the ferrocenyl borenium ions (see below), may nevertheless provide the very extra stability needed to isolate the free Lewis acids (compare the case of the $[\mathbf{D}–NTf_2]^- \leftrightarrow \mathbf{D} + [NTf_2]^-$ equilibrium shown in Fig. 1).

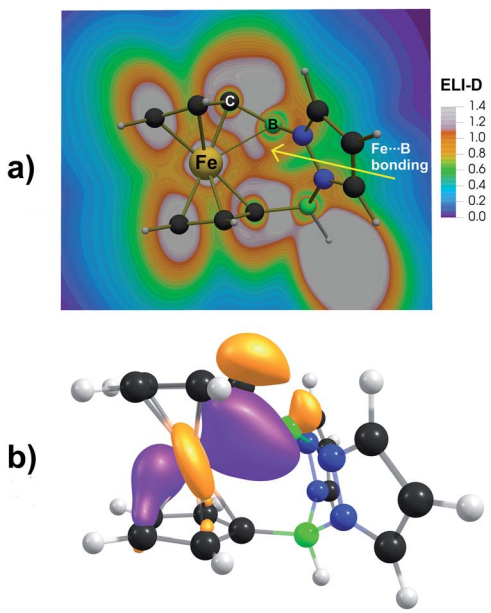

Fig. 3 (a) Electron localizability indicator (ELI-D) analysis of bonding in $[\mathbf{2}]^+$. The selected plane includes the Fe and two B atoms. The gray-white regions represent ELF maxima (bonding attractors), showing a donor–acceptor Fe···B interaction. (b) Natural localized molecular orbital (NLMO) corresponding to a 3c2e bond between Fe(II), B(sp^2), and the adjacent C_i atom in $[\mathbf{2}]^+$ (isosurface plot: ±0.05 au). NLMO composition is as follows: 51% Fe (99% d), 15% B (10% s, 90% p), 26% C (99% p). A similar NLMO picture was obtained for $[\mathbf{2Me}]^+$ with the following composition: 50% Fe (99% d), 14% B (10% s, 90% p), 28% C (99% p).

Assessment of the Lewis acidity of the borenium cation $[\mathbf{2}]^+$ by the Gutmann–Beckett NMR method, competition experiments with $B(C_6F_5)_3$ and computational studies

The sterically less encumbered borenium-ion derivative $[\mathbf{2}]^+$ was selected for a comparative assessment of Lewis acidities. We first determined the acceptor number (AN) of $[\mathbf{2}]^+$ on the scale developed by Gutmann and Beckett.[35] To this end, mixtures of $[\mathbf{2}][B(C_6F_5)_4]$ and Et_3PO were prepared in CD_2Cl_2 and $^{31}P\{^1H\}$ NMR spectra were recorded (see the ESI† for full details). We consistently observed a resonance at $\delta(^{31}P)$ = 91.0 ppm for the adduct $[\mathbf{2}\cdot OPEt_3][B(C_6F_5)_4]$. The signal is shifted to lower field by 40.7 ppm and 50.0 ppm, compared to the resonance of pure Et_3PO in CD_2Cl_2 (50.3 ppm) or *n*-hexane (41.0 ppm), respectively. From these data, an acceptor number AN($[\mathbf{2}]^+$) = 111 was calculated, which is significantly higher than the acceptor number of $B(C_6F_5)_3$ (AN = 77–82; CD_2Cl_2), higher than the acceptor numbers of so far reported Fc-borenium ions (*cf.* Table S7 in ESI†), and close to that of neat BBr_3 (AN = 109) or BI_3 (AN = 115).[36]

The pyridine adduct $[\mathbf{2}\cdot py][B(C_6F_5)_4]$ was synthesized on a preparative scale and characterized by NMR-spectroscopy and X-ray crystallography (Scheme 2). Five ^{1}H and five ^{13}C resonances are observed for the pyridine ligand in the corresponding room-temperature NMR spectra, demonstrating a sterically restricted rotation about the B–N(py) bond on the NMR time scale (CD_2Cl_2). The *p*-CH group of the coordinated pyridine molecule should be least affected by magnetic anisotropy effects originating from the surrounding π-electron clouds. Its continuous deshielding upon going from free pyridine ($\delta(^1H)/\delta(^{13}C)$ = 7.67/136.1 ppm)[11b] to $B(C_6F_5)_3\cdot py$ (8.21/143.2 ppm)[11b] and $[\mathbf{2}\cdot py][B(C_6F_5)_4]$ (8.56/147.8 ppm) therefore indicates increasing charge polarization induced by increasingly strong N–B donor–acceptor binding (*cf.* [Hpy]Cl: 8.51/146.1 ppm (ref. 11b)). Consistent with this, the N(py)–B bond in $[\mathbf{2}\cdot py][B(C_6F_5)_4]$ (1.603(3) Å) is shorter than that in $B(C_6F_5)_3\cdot py$ (1.614(2) Å,[37] 1.628(2) Å (ref. 38)), but identical to the N–B bond in the adducts $[\mathbf{B}\cdot py][O_3SCF_3]$ (1.599(4) Å (ref. 11b)) and $B(C_6F_5)_3\cdot DMAP$, which contains the stronger donor *p*-dimethylaminopyridine (1.602(6) Å (ref. 39)).

We also performed competition experiments using the combinations $[\mathbf{2}\cdot Do][B(C_6F_5)_4]/B(C_6F_5)_3$ and $[\mathbf{2}][B(C_6F_5)_4]/B(C_6F_5)_3\cdot Do$

© 2022 The Author(s). Published by the Royal Society of Chemistry

Open Access Article. Published on 07 diciembre 2021. Downloaded on 21/04/2026 15:29:20.
This article is licensed under a Creative Commons Attribution-NonCommercial 3.0 Unported Licence.

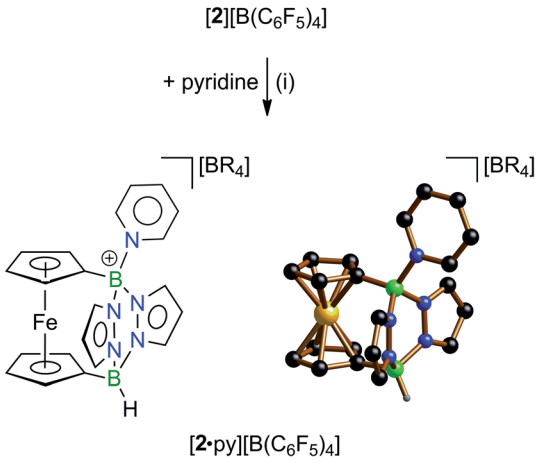

Scheme 2 Synthesis and solid-state structure of the pyridine adduct [2·py][B(C$_6$F$_5$)$_4$]; C-bonded H atoms and the [B(C$_6$F$_5$)$_4$]$^-$ anion are omitted for clarity. Reagents and conditions: (i) $CHCl_3$, room temperature. R = C_6F_5.

in CD_2Cl_2 (Do = Et_3PO or pyridine). Irrespective of the ligand employed, we found that the transfer of Do from B(C$_6$F$_5$)$_3$ to [2]$^+$ was faster and occurred to a much higher extent than *vice versa*, which clearly points to a higher Lewis acidity of [2]$^+$ compared to B(C$_6$F$_5$)$_3$ (see the ESI† for plots of corresponding NMR spectra). A quantitative determination of exchange-equilibrium constants was not possible, because [2][B(C$_6$F$_5$)$_4$] is not stable over the long term toward B(C$_6$F$_5$)$_3$. An observed slow increase in the amount of B(C$_6$F$_5$)$_3$·Do over the course of several days may therefore well be preceded by a slow B(C$_6$F$_5$)$_3$-induced degradation of [2]$^+$/[2·Do]$^+$ and subsequent trapping of the released ligand by B(C$_6$F$_5$)$_3$.

To confirm the exceptionally strong Lewis acidity of [2]$^+$ indicated by the above experiments, we compared the Et_3PO affinities and Gutmann–Beckett acceptor numbers for [2]$^+$/[**2Me**]$^+$, the Ru/Os congeners of [2]$^+$, a series of structurally related neutral/ionic Fc–B Lewis acids, and variously substituted boranes also on the basis of quantum-chemical calculations (Table S7 and Fig. S67, S68†). When taking into account the solvation and counterion effects (where appropriate), we observe a very good correlation between experimental and computed ^{31}P NMR shifts for a range of 28 Lewis acid adducts with Et_3PO (Table S7 and Fig. S67†); the linear regression is improved almost to perfection ($R^2 = 0.991$) when the data points for the boron trihalides BX_3 are omitted (X = F, Cl, Br, I). In accordance with the experimental NMR studies, the DFT calculations indicate that [2]$^+$ is one of the strongest Lewis acids among hitherto reported boron-containing species.

Given that the assessment of Lewis acidity based on the Gutmann–Beckett method is sometimes under criticism, in particular when comparing the Lewis acidity of ionic and neutral borane species,[40] we also calculated the F$^-$-ion affinities (FIAs) for the above series of Lewis acids (Table S9†). The calculations were performed along the lines of Christe's method using F_2CO as the standard, which avoids the theoretical treatment of free F$^-$ in the gas phase.[41,42] Fig. S69 and S70† show that there is a reasonably good correlation between the computed FIAs and the ^{31}P NMR shifts, acceptor numbers, and Et_3PO affinities for all compounds studied. Thus, also according to the FIAs, [2]$^+$ is one of the strongest Lewis acids among the boron-containing systems: Apart from Ingleson's transient [CatB][CbBr$_6$] (Cat = catecholato, [CbBr$_6$]$^-$ = [*closo*-1-H-CB$_{11}$H$_5$Br$_6$]$^-$),[43] [2]$^+$ outperforms all neutral and ionic Fc–B species as well as variously substituted boranes and borenium ions, including Corey's oxazaborolidinium cations [C]$^+$,[12] and Jäkle's borenium Lewis acids.[40] A borderline case is the hypothetical free 9-phosphonium-10-boratriptycene cation, which could not yet be isolated (*cf.* the structural motif of **D** featuring a [PH]$^+$ rather than a CH group at the bridgehead position; Fig. 1):[17a] while the computed Gutmann–Beckett acceptor number of [2]$^+$ is higher than that of 9-phosphonium-10-boratriptycene (AN_{calcd} = 110 *vs.* 83; Table S7†), the FIA of [2]$^+$ is lower (FIA = 396 *vs.* 474 kJ mol^{-1}; Table S9†).

We finally note that replacing the Fe(II) center in [2]$^+$ with Ru(II) or Os(II) leads to more shielded ^{31}P nuclei in corresponding Et_3PO adducts, which indicates a reduced Lewis acidity of the B$^+$ centers, consistent with stronger M → B donation (see above).

Optoelectronic properties of 1/[2][B(C$_6$F$_5$)$_4$] and 1Me/[2Me][B(C$_6$F$_5$)$_4$]

Cyclic voltammograms and UV/vis spectra were recorded in CH_2Cl_2 at room temperature. The Fe(II)/Fe(III) transitions of **1** and **1Me** occur at halve-wave potentials of $E_{1/2}$ = −0.23 V and −0.32 V, respectively (*vs.* FcH/FcH$^+$). Their 1,1′-fc moieties are therefore easier to oxidize than the reference compound ferrocene, indicating a net electron-donating effect of the two tetracoordinated B substituents. Jäkle *et al.* reported on a pronounced Lewis acidity enhancement of neutral diboradiferrocenes upon oxidation of their 1,2-ferrocenylene moieties.[44] In a similar vein, we have also attempted the Fe-centered oxidation of [2][B(C$_6$F$_5$)$_4$] and [**2Me**][B(C$_6$F$_5$)$_4$] with the goal of generating dicationic borenium ions, but have not been successful so far. The longest-wavelength absorptions of **1** and **1Me** in CH_2Cl_2 are broad and appear at λ_{max} = 451 nm, near the most bathochromic band in the UV-vis spectrum of parent ferrocene (441 nm).[45] The experimentally determined absorption maximum is well reproduced by TD-DFT calculations on **1**, which predict a transition at λ_{max}(calc) = 447 nm (f_{OSC} = 0.001), attributable to a charge transfer from the 1,1′-fc unit to the pyrazole rings (HOMO−1 → LUMO). [2][B(C$_6$F$_5$)$_4$] and [**2Me**][B(C$_6$F$_5$)$_4$] show their longest-wavelength absorptions at λ_{max} = 378 and 391 nm, respectively (CH_2Cl_2; Fig. 4). According to TD-DFT calculations, the first absorption peak of [2]$^+$ at λ_{max} = 378 nm (λ_{max}(calc) = 383 nm; f_{OSC} = 0.004) is mainly associated with a charge transfer from Fe(II) d-orbitals (HOMO−2) to the Cp rings (LUMO+1). The second intense peak at 309 nm (λ_{max}(calc) = 317 nm; f_{OSC} = 0.082) can be attributed to an Fe(II) → B_2pz_2 (HOMO−2 → LUMO) transfer (Fig. 4). However, the transferred electron density accumulates predominantly at the pz moieties, and the charge at the B$^+$ center does not change much upon excitation (Table S12†) due to the delocalized nature of the corresponding MOs (ground-state [2]$^+$: q(B(2p)) = 0.90 e$^-$, excited-state [2]$^+$: q(B(2p)) = 0.91 e$^-$).

© 2022 The Author(s). Published by the Royal Society of Chemistry

Open Access Article. Published on 07 diciembre 2021. Downloaded on 21/04/2026 15:29:20.
This article is licensed under a Creative Commons Attribution-NonCommercial 3.0 Unported Licence.

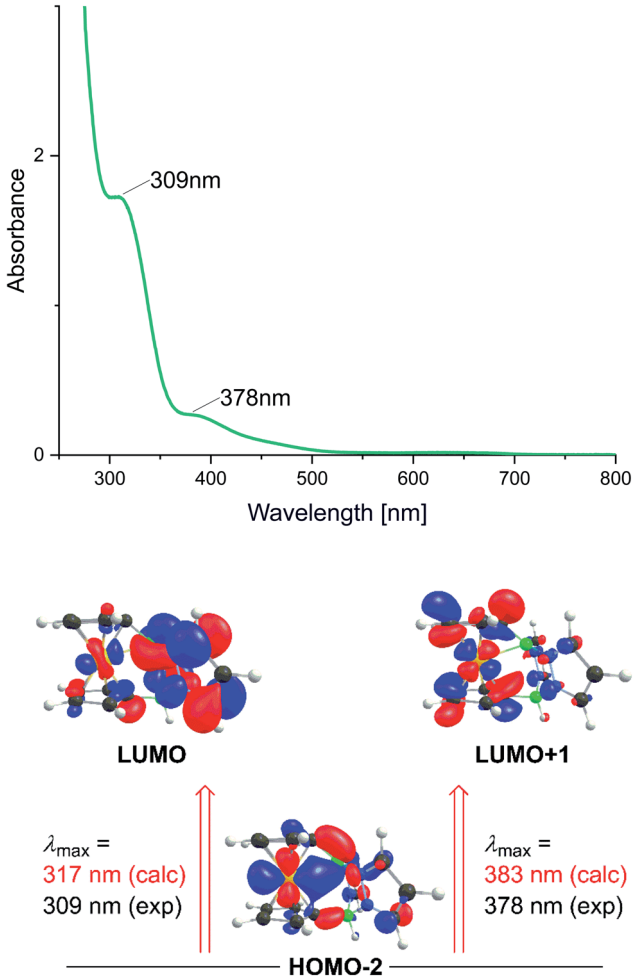

Fig. 4 Top: experimentally determined UV/vis absorption spectrum of [**2**][$B(C_6F_5)_4$] in CH_2Cl_2. Bottom: computed key molecular orbitals of [**2**]$^+$ and lowest energy electronic transitions (TD-DFT PBE0-10HF/def2-TZVP/CH_2Cl_2).

Conclusions

By exploiting the facile self-assembly of the pyrazabole scaffold, we have devised a straightforward route to boratriptycene-type precursors that have two pyrazole bridges and one 1,1′-ferrocenylene linker between two bridgehead BH moieties (**1**, **1Me**). H^- abstraction with the $[Ph_3C]^+$ cation generates bridgehead borenium cations of exceptional Lewis acidity that can nevertheless be isolated in free form ([**2**][$B(C_6F_5)_4$], [**2Me**][$B(C_6F_5)_4$]). A weak Fe–B(sp^2) through-space interaction likely assists in stabilizing the systems without appreciably diminishing their electron-pair affinities. Although the borenium centers of [**2**]$^+$ and [**2Me**]$^+$ adopt trigonal-planar configurations (X-ray crystallography, DFT calculations), huge dips of the B atoms with respect to their attached Cp rings indicate pretensioned 'entatic' states of the molecules,[46] which should significantly promote Lewis acid–base pairing. Since a plethora of pyrazole derivatives are available, the degree of steric protection of the electrophilic borenium center can be varied easily (*cf.* [**2**]$^+$ with pyrazole bridges *vs.* [**2Me**]$^+$ with bulky 3,5-dimethylpyrazole bridges). By using chiral substituents in the 3,5-positions of the pyrazole rings, even chiral Lewis acids should be within reach. As an outlook, we note that an exchange of Fe for Os would lead to a related Lewis acid that is computed to exhibit a distinct Os(III)/B$^\bullet$ character in its relaxed triplet excited state and thus could open new avenues for exploring the evolving chemistry of *in situ*-generated boron radicals.[47]

Data availability

Experimental and computational data associated with this article have been provided in the ESI.†

Author contributions

M. H. synthesized and characterized all compounds. J. N. and P. H. performed all quantum-chemical calculations. A. O. and V. S. recorded and interpreted the Mössbauer spectra. M. B. performed the X-ray crystal structure analyses. H.-W. L. and M. W. supervised the project. The manuscript was written by M. W. and P. H. and edited by all the co-authors.

Conflicts of interest

There are no conflicts of interest to declare.

Acknowledgements

M. W. and M. H. thank the Deutsche Forschungsgemeinschaft (DFG, German Research Foundation) for financial support (WA 864/6-1). V. S. acknowledges the support of the DFG through TRR 88 142808194 3MET. J. N. and P. H. acknowledge the support by the Slovak Research and Development Agency (grant no. APVV-17-0324), the Grant Agency of the Ministry of Education of the Slovak Republic (VEGA project no. 1/0712/18), and by the European Union's Horizon 2020 research and innovation programme under grant no. 810701 (LAMatCU).

Notes and references

1 (*a*) W. E. Piers and T. Chivers, *Chem. Soc. Rev.*, 1997, **26**, 345–354; (*b*) E. Y.-X. Chen and T. J. Marks, *Chem. Rev.*, 2000, **100**, 1391–1434; (*c*) M. Bochmann, S. J. Lancaster, M. D. Hannant, A. Rodriguez, M. Schormann, D. A. Walker and T. J. Woodman, *Pure Appl. Chem.*, 2003, **75**, 1183–1195; (*d*) G. Erker, *Chem. Commun.*, 2003, 1469–1476; (*e*) W. E. Piers, *Adv. Organomet. Chem.*, 2005, **52**, 1–76; (*f*) F. Jäkle, in *Encyclopedia of Inorganic Chemistry*, ed. R. B. King, R. H. Crabtree, C. M. Lukehart, D. A. Atwood and R. A. Scott, John Wiley & Sons, Ltd, Chichester, UK, 2006.

2 (*a*) D. W. Stephan and G. Erker, *Angew. Chem., Int. Ed.*, 2010, **49**, 46–76; (*b*) D. W. Stephan, *J. Am. Chem. Soc.*, 2015, **137**, 10018–10032; (*c*) D. W. Stephan, *Acc. Chem. Res.*, 2015, **48**, 306–316; (*d*) A. R. Jupp and D. W. Stephan, *Trends Chem.*, 2019, **1**, 35–48.

3 (*a*) L. A. Mück, A. Y. Timoshkin and G. Frenking, *Inorg. Chem.*, 2012, **51**, 640–646; (*b*) A. Y. Timoshkin and

© 2022 The Author(s). Published by the Royal Society of Chemistry

Open Access Article. Published on 07 diciembre 2021. Downloaded on 21/04/2026 15:29:20.
This article is licensed under a Creative Commons Attribution-NonCommercial 3.0 Unported Licence.

K. Morokuma, *Phys. Chem. Chem. Phys.*, 2012, **14**, 14911–14916; (*c*) T. M. Gilbert, *Dalton Trans.*, 2012, **41**, 9046–9055; (*d*) E. I. Davydova, T. N. Sevastianova and A. Y. Timoshkin, *Coord. Chem. Rev.*, 2015, **297–298**, 91–126.

4 (*a*) P. A. Chase, W. E. Piers and B. O. Patrick, *J. Am. Chem. Soc.*, 2000, **122**, 12911–12912; (*b*) C. Fan, W. E. Piers and M. Parvez, *Angew. Chem., Int. Ed.*, 2009, **48**, 2955–2958; (*c*) A. Y. Houghton, V. A. Karttunen, W. E. Piers and H. M. Tuononen, *Chem. Commun.*, 2014, **50**, 1295–1298; (*d*) A. Y. Houghton, J. Hurmalainen, A. Mansikkamäki, W. E. Piers and H. M. Tuononen, *Nat. Chem.*, 2014, **6**, 983–988; (*e*) J. L. Carden, A. Dasgupta and R. L. Melen, *Chem. Soc. Rev.*, 2020, **49**, 1706–1725.

5 (*a*) A. G. Massey and A. J. Park, *J. Organomet. Chem.*, 1964, **2**, 245–250; (*b*) A. G. Massey and A. J. Park, *J. Organomet. Chem.*, 1966, **5**, 218–225.

6 A. E. Ashley, T. J. Herrington, G. G. Wildgoose, H. Zaher, A. L. Thompson, N. H. Rees, T. Krämer and D. O'Hare, *J. Am. Chem. Soc.*, 2011, **133**, 14727–14740.

7 (*a*) J. Landmann, F. Keppner, D. B. Hofmann, J. A. P. Sprenger, M. Häring, S. H. Zottnick, K. Müller-Buschbaum, N. V. Ignat'ev and M. Finze, *Angew. Chem., Int. Ed.*, 2017, **56**, 2795–2799; (*b*) E. L. Bennett, E. J. Lawrence, R. J. Blagg, A. S. Mullen, F. MacMillan, A. W. Ehlers, D. J. Scott, J. S. Sapsford, A. E. Ashley, G. G. Wildgoose and J. C. Slootweg, *Angew. Chem., Int. Ed.*, 2019, **58**, 8362–8366.

8 (*a*) T. W. Hudnall, C.-W. Chiu and F. P. Gabbaï, *Acc. Chem. Res.*, 2009, **42**, 388–397; (*b*) H. Zhao, L. A. Leamer and F. P. Gabbaï, *Dalton Trans.*, 2013, **42**, 8164–8178.

9 Y. Kim and F. P. Gabbaï, *J. Am. Chem. Soc.*, 2009, **131**, 3363–3369.

10 For selected examples of conceptually related positively charged boron Lewis acids, see: (*a*) C. Dusemund, K. R. A. Samankumara Sandanayake and S. Shinkai, *J. Chem. Soc., Chem. Commun.*, 1995, 333–334; (*b*) C.-W. Chiu and F. P. Gabbaï, *J. Am. Chem. Soc.*, 2006, **128**, 14248–14249; (*c*) T. Agou, J. Kobayashi and T. Kawashima, *Inorg. Chem.*, 2006, **45**, 9137–9144; (*d*) T. W. Hudnall and F. P. Gabbaï, *J. Am. Chem. Soc.*, 2007, **129**, 11978–11986; (*e*) M. H. Lee, T. Agou, J. Kobayashi, T. Kawashima and F. P. Gabbaï, *Chem. Commun.*, 2007, 1133–1135; (*f*) K. Venkatasubbaiah, I. Nowik, R. H. Herber and F. Jäkle, *Chem. Commun.*, 2007, 2154–2156; (*g*) G. C. Welch, L. Cabrera, P. A. Chase, E. Hollink, J. D. Masuda, P. Wei and D. W. Stephan, *Dalton Trans.*, 2007, 3407–3414; (*h*) J. K. Day, C. Bresner, N. D. Coombs, I. A. Fallis, L.-L. Ooi and S. Aldridge, *Inorg. Chem.*, 2008, **47**, 793–804; (*i*) T. W. Hudnall, Y. M. Kim, M. W. Bebbington, D. Bourissou and F. P. Gabbaï, *J. Am. Chem. Soc.*, 2008, **130**, 10890–10891; (*j*) Y. Kim, H. Zhao and F. P. Gabbaï, *Angew. Chem., Int. Ed.*, 2009, **48**, 4957–4960; (*k*) D. Cao, H. Zhao and F. P. Gabbaï, *New J. Chem.*, 2011, **35**, 2299–2305.

11 (*a*) A. Schnurr, H. Vitze, M. Bolte, H.-W. Lerner and M. Wagner, *Organometallics*, 2010, **29**, 6012–6019; (*b*) A. Schnurr, M. Bolte, H.-W. Lerner and M. Wagner, *Eur. J. Inorg. Chem.*, 2012, **2012**, 112–120.

12 (*a*) E. J. Corey, T. Shibata and T. W. Lee, *J. Am. Chem. Soc.*, 2002, **124**, 3808–3809; (*b*) D. H. Ryu, T. W. Lee and E. J. Corey, *J. Am. Chem. Soc.*, 2002, **124**, 9992–9993; (*c*) G. Zhou and E. J. Corey, *J. Am. Chem. Soc.*, 2005, **127**, 11958–11959.

13 (*a*) A. Chardon, A. Osi, D. Mahaut, A. Ben Saida and G. Berionni, *Synlett*, 2020, **31**, 1639–1648; (*b*) K. T. Giju, A. K. Phukan and E. D. Jemmis, *Angew. Chem., Int. Ed.*, 2003, **42**, 539–542.

14 B. M. Mikhailov, *Pure Appl. Chem.*, 1983, **55**, 1439–1452.

15 (*a*) S. Y. Erdyakov, A. V. Ignatenko, T. V. Potapova, K. A. Lyssenko, M. E. Gurskii and Y. N. Bubnov, *Org. Lett.*, 2009, **11**, 2872–2875; (*b*) M. E. Gurskii, G. D. Kolomnikova, S. V. Baranin and Y. N. Bubnov, *Mendeleev Commun.*, 2018, **28**, 366–368.

16 A. Chardon, A. Osi, D. Mahaut, T.-H. Doan, N. Tumanov, J. Wouters, L. Fusaro, B. Champagne and G. Berionni, *Angew. Chem., Int. Ed.*, 2020, **59**, 12402–12406.

17 For **D**-type compounds containing (a) a P atom or (b) an S^+ cation instead of the CH group at the second bridgehead position, see: (*a*) A. Ben Saida, A. Chardon, A. Osi, N. Tumanov, J. Wouters, A. I. Adjieufack, B. Champagne and G. Berionni, *Angew. Chem., Int. Ed.*, 2019, **58**, 16889–16893; (*b*) A. Osi, D. Mahaut, N. Tumanov, L. Fusaro, J. Wouters, B. Champagne, A. Chardon and G. Berionni, *Angew. Chem., Int. Ed.*, 2021, DOI: 10.1002/anie.202112342. For related Lewis base adducts of 1-borabarrelenes, see: (*c*) T. K. Wood, W. E. Piers, B. A. Keay and M. Parvez, *Org. Lett.*, 2006, **8**, 2875–2878.

18 Y. V. Vishnevskiy, M. A. Abaev, A. N. Rykov, M. E. Gurskii, P. A. Belyakov, S. Y. Erdyakov, Y. N. Bubnov and N. W. Mitzel, *Chem.–Eur. J.*, 2012, **18**, 10585–10594.

19 (*a*) B. Wrackmeyer, W. Milius, O. L. Tok and Y. N. Bubnov, *Chem.–Eur. J.*, 2002, **8**, 1537–1543; (*b*) C. E. Wagner, J.-S. Kim and K. J. Shea, *J. Am. Chem. Soc.*, 2003, **125**, 12179–12195.

20 (*a*) A. Appel, F. Jäkle, T. Priermeier, R. Schmid and M. Wagner, *Organometallics*, 1996, **15**, 1188–1194; (*b*) K. Ma, M. Scheibitz, S. Scholz and M. Wagner, *J. Organomet. Chem.*, 2002, **652**, 11–19; (*c*) M. Scheibitz, M. Bolte, J. W. Bats, H.-W. Lerner, I. Nowik, R. H. Herber, A. Krapp, M. Lein, M. C. Holthausen and M. Wagner, *Chem.–Eur. J.*, 2005, **11**, 584–603; (*d*) L. Kaufmann, H. Vitze, M. Bolte, H. W. Lerner and M. Wagner, *Organometallics*, 2008, **27**, 6215–6221; (*e*) U. D. Eckensberger, K. Kunz, M. Bolte, H.-W. Lerner and M. Wagner, *Organometallics*, 2008, **27**, 764–768; (*f*) H. Braunschweig, I. Fernández, G. Frenking and T. Kupfer, *Angew. Chem., Int. Ed.*, 2008, **47**, 1951–1954; (*g*) H. Braunschweig, C.-W. Chiu, D. Gamon, M. Kaupp, I. Krummenacher, T. Kupfer, R. Müller and K. Radacki, *Chem.–Eur. J.*, 2012, **18**, 11732–11746.

21 (*a*) M. Fontani, F. Peters, W. Scherer, W. Wachter, M. Wagner and P. Zanello, *Eur. J. Inorg. Chem.*, 1998, **1998**, 1453–1465; (*b*) M. Grosche, E. Herdtweck, F. Peters and M. Wagner, *Organometallics*, 1999, **18**, 4669–4672; (*c*) M. Scheibitz,

Open Access Article. Published on 07 diciembre 2021. Downloaded on 21/04/2026 15:29:20.
This article is licensed under a Creative Commons Attribution-NonCommercial 3.0 Unported Licence.

J. W. Bats, M. Bolte and M. Wagner, *Eur. J. Inorg. Chem.*, 2003, **2003**, 2049–2053.

22 (*a*) F. Jäkle, T. Priermeier and M. Wagner, *J. Chem. Soc., Chem. Commun.*, 1995, 1765–1766; (*b*) F. Jäkle, M. Mattner, T. Priermeier and M. Wagner, *J. Organomet. Chem.*, 1995, **502**, 123–130; (*c*) E. Herdtweck, F. Jäkle, G. Opromolla, M. Spiegler, M. Wagner and P. Zanello, *Organometallics*, 1996, **15**, 5524–5535; (*d*) F. Jäkle, T. Priermeier and M. Wagner, *Organometallics*, 1996, **15**, 2033–2040; (*e*) E. Herdtweck, F. Jäkle and M. Wagner, *Organometallics*, 1997, **16**, 4737–4745.

23 For review articles on borocations, see: (*a*) D. Franz and S. Inoue, *Chem.–Eur. J.*, 2019, **25**, 2898–2926; (*b*) M. J. Ingleson, in *Topics in Organomet. Chem.*, Springer, 2015, vol. 49, pp. 39–71; (*c*) T. S. de Vries, A. Prokofjevs and E. Vedejs, *Chem. Rev.*, 2012, **112**, 4246–4282; (*d*) W. E. Piers, S. C. Bourke and K. D. Conroy, *Angew. Chem., Int. Ed.*, 2005, **44**, 5016–5036.

24 For selected adducts of cage-like boron Lewis acids that have been prepared from tripodal triamido or triaryloxy ligands to establish BN_3 or BO_3 environments, see: (*a*) M. Yasuda, S. Yoshioka, S. Yamasaki, T. Somyo, K. Chiba and A. Baba, *Org. Lett.*, 2006, **8**, 761–764; (*b*) H. Zhu and E. Y. Chen, *Inorg. Chem.*, 2007, **46**, 1481–1487; (*c*) H. Nakajima, M. Yasuda, R. Takeda and A. Baba, *Angew. Chem., Int. Ed.*, 2012, **51**, 3867–3870; (*d*) A. Konishi, K. Nakaoka, H. Nakajima, K. Chiba, A. Baba and M. Yasuda, *Chem.–Eur. J.*, 2017, **23**, 5219–5223.

25 Boron compounds of the forms $(C_6F_5)_nB(OC_6F_5)_{3-n}$ $(n = 0–2)$ are also known. Their Lewis acidities with respect to Et_3PO increase as n decreases, which is due to the negative inductive effect of the electronegative O atoms. In these particular cases, this −I effect is not compensated by strong O=B π-backbonding, since the oxygen-bonded C_6F_5 substituents themselves have a strong π-electron withdrawing character: (*a*) D. Naumann, H. Butler and R. Gnann, *Z. Anorg. Allg. Chem.*, 1992, **618**, 74–76; (*b*) G. J. P. Britovsek, J. Ugolotti and A. J. P. White, *Organometallics*, 2005, **24**, 1685–1691.

26 M. Scheibitz, H. Li, J. Schnorr, A. Sánchez Perucha, M. Bolte, H.-W. Lerner, F. Jäkle and M. Wagner, *J. Am. Chem. Soc.*, 2009, **131**, 16319–16329.

27 Comparable hydride-abstraction reactions from pentamethylazaferrocene–borane adducts have been described: B. Bentivegna, C. I. Mariani, J. R. Smith, S. Ma, A. L. Rheingold and T. J. Brunker, *Organometallics*, 2014, **33**, 2820–2830.

28 A. Iida, A. Sekioka and S. Yamaguchi, *Chem. Sci.*, 2012, **3**, 1461–1466.

29 (*a*) B. Wrackmeyer, *Z. Anorg. Allg. Chem.*, 2015, **641**, 2525–2529; (*b*) B. Wrackmeyer, B. Schwarze and W. Milius, *Inorg. Chim. Acta*, 1996, **241**, 87–93. The conclusion that the B–N bonds in this compound have essentially single-bond character is based on the following considerations (i) the electron lone pairs on the N atoms contribute mainly to the heteroaromatic systems, which would be perturbed by B=N π bonding, (ii) the Me_2pyr rings are strongly twisted against the BN_3 plane (dihedral angles = 36.7°, 48.5°, 50.8°), (iii) three nitrogen lone pairs would compete for one vacant boron 2p orbital, which necessarily reduces any double-bond character of the individual B–N bonds.

30 H. Nöth and B. Wrackmeyer, Nuclear Magnetic Resonance Spectroscopy of Boron Compounds, in *NMR – Basic Principles and Progress*, ed. P. Diehl, E. Fluck and R. Kosfeld, Springer, Berlin, Heidelberg, New York, 1978.

31 T. Renk, W. Ruf and W. Siebert, *J. Organomet. Chem.*, 1976, **120**, 1–25.

32 K. Müther, P. Hrobárik, V. Hrobáriková, M. Kaupp and M. Oestreich, *Chem.–Eur. J.*, 2013, **19**, 16579–16594.

33 (*a*) D. F. Shriver, *Acc. Chem. Res.*, 1970, **3**, 231–238; (*b*) H. Braunschweig, C. Kollann and D. Rais, *Angew. Chem., Int. Ed.*, 2006, **45**, 5254–5274; (*c*) A. Amgoune and D. Bourissou, *Chem. Commun.*, 2011, **47**, 859–871; (*d*) H. Braunschweig and R. D. Dewhurst, *Dalton Trans.*, 2011, **40**, 549–558; (*e*) H. Braunschweig, R. D. Dewhurst and A. Schneider, *Chem. Rev.*, 2010, **110**, 3924–3957.

34 (*a*) J. S. Figueroa, J. G. Melnick and G. Parkin, *Inorg. Chem.*, 2006, **45**, 7056–7058; (*b*) M. Sircoglou, S. Bontemps, G. Bouhadir, N. Saffon, K. Miqueu, W. Gu, M. Mercy, C.-H. Chen, B. M. Foxman, L. Maron, O. V. Ozerov and D. Bourissou, *J. Am. Chem. Soc.*, 2008, **130**, 16729–16738.

35 (*a*) V. Gutmann, *Coord. Chem. Rev.*, 1976, **18**, 225–255; (*b*) M. A. Beckett, D. S. Brassington, S. J. Coles and M. B. Hursthouse, *Inorg. Chem. Commun.*, 2000, **3**, 530–533.

36 I. B. Sivaev and V. I. Bregadze, *Coord. Chem. Rev.*, 2014, **270–271**, 75–88.

37 K. Tanifuji, S. Tajima, Y. Ohki and K. Tatsumi, *Inorg. Chem.*, 2016, **55**, 4512–4518.

38 F. Focante, P. Mercandelli, A. Sironi and L. Resconi, *Coord. Chem. Rev.*, 2006, **250**, 170–188.

39 M. J. G. Lesley, A. Woodward, N. J. Taylor, T. B. Marder, I. Cazenobe, I. Ledoux, J. Zyss, A. Thornton, D. W. Bruce and A. K. Kakkar, *Chem. Mater.*, 1998, **10**, 1355–1365.

40 (*a*) J. Chen, R. A. Lalancette and F. Jäkle, *Chem. Commun.*, 2013, **49**, 4893–4895; (*b*) P. Erdmann and L. Greb, *Angew. Chem., Int. Ed.*, 2021, DOI: 10.1002/anie.202114550.

41 K. O. Christe, D. A. Dixon, D. McLemore, W. W. Wilson, J. A. Sheehy and J. A. Boatz, *J. Fluorine Chem.*, 2000, **101**, 151–153.

42 The inclusion of an implicit solvation model is necessary to obtain reliable FIAs when comparing neutral and ionic boron-based Lewis acids in condensed (solution) phase to reflect the experimentally observed trends (the gas-phase results overestimate the Lewis acidities of cationic species due to unshielded Coulomb attraction and charge-effect contributions; Tables S8 vs. S9†).

43 A. Del Grosso, R. G. Pritchard, C. A. Muryn and M. J. Ingleson, *Organometallics*, 2010, **29**, 241–249.

44 K. Venkatasubbaiah, L. N. Zakharov, W. S. Kassel, A. L. Rheingold and F. Jäkle, *Angew. Chem., Int. Ed.*, 2005, **44**, 5428–5433.

45 H. B. Gray, Y. S. Sohn and N. Hendrickson, *J. Am. Chem. Soc.*, 1971, **93**, 3603–3612.

© 2022 The Author(s). Published by the Royal Society of Chemistry

Open Access Article. Published on 07 diciembre 2021. Downloaded on 21/04/2026 15:29:20.
This article is licensed under a Creative Commons Attribution-NonCommercial 3.0 Unported Licence.

46 (*a*) B. L. Vallee and R. J. P. Williams, *Proc. Natl. Acad. Sci. U. S. A.*, 1968, **59**, 498–505; (*b*) R. J. P. Williams, *Eur. J. Biochem.*, 1995, **234**, 363–381.

47 (*a*) J. T. Henthorn and T. Agapie, *Angew. Chem., Int. Ed.*, 2014, **53**, 12893–12896; (*b*) L. L. Liu, L. L. Cao, Y. Shao and D. W. Stephan, *J. Am. Chem. Soc.*, 2017, **139**, 10062–10071; (*c*) X. Tao, C. G. Daniliuc, R. Knitsch, M. R. Hansen, H. Eckert, M. Lübbesmeyer, A. Studer, G. Kehr and G. Erker, *Chem. Sci.*, 2018, **9**, 8011–8018.

© 2022 The Author(s). Published by the Royal Society of Chemistry